ISTITUTO NAZIONALE DI FISICA NUCLEARE

Sezione di Bologna

INFN/AE-88/1
1 Marzo 1988

D. Bollini,T. Camporesi, F.R. Cavallo, C. Chiccoli, P. Giusti, F.L. Navarria, and P. Pasini:

Simulations for the delphi HPC second level trigger

Servizio Documentazione
dei Laboratori Nazionali di Frascati

INFN - ISTITUTO NAZIONALE DI FISICA NUCLEARE
Sezione di BOLOGNA

INFN/AE-88/1
1 Marzo 1988

SIMULATIONS FOR THE DELPHI HPC SECOND LEVEL TRIGGER

D. Bollini, T. Camporesi, F.R. Cavallo, C. Chiccoli, P. Giusti, F.L. Navarria and P. Pasini*
Dipartimento di Fisica dell'Univ. ,I.N.F.N. Sez. di BOLOGNA and C.N.A.F.,
Via Irnerio 46, 40126 BOLOGNA, ITALY
** CERN Fellow*

1 - INTRODUCTION

The HPC second level trigger must perform the following tasks:

- measure the deposited energy according to a given (Θ, Φ) granularity;
- compare the measured values with a low and a high energy threshold and count the "low" and "high" hits multiplicity;
- encode the multiplicity information in four bits; two for the low hits (EMBLLO) and two for the high hits (EMBLHI) so that multiplicities $0, 1, 2$ and > 2 are defined;
- calculate the total energy released in the HPC detector which is to be compared with a low and a high energy threshold to set, accordingly, two bits: EMBLTELO, EMBLTEHI;
- save the information of which (Θ, Φ) cells have been hit to be used by the 3rd level trigger processor.

The HPC detector is constituted by 144 modules: 24 modules in Φ and 6 modules along Θ. Within a total drift time of max 16 μsec each module is read out by 128 cathode pads which provide, together with the drift time information, the good space localizations of the energy depositions required at the final off-line analysis level.

For the second level trigger, which must give an answer within 35 μsec from the beam cross over (BCO) time, however, such a number of channels is too large and an appropriate reduction may be obtained, a priori, either by performing analog sums of the pad signals or by reading out the 39 anode wires of the HPC module. The cathode pad layout and the anode wires are shown in Fig. 1.

For what concerns the (Θ, Φ) granularity of the HPC second level trigger, in order to reduce the complexity of the system, it was originally proposed [1] to measure the energy in each separate HPC module without making use of the information on the longitudinal development of the showers and on the drift time.

module without making use of the information on the longitudinal development of the showers and on the drift time.

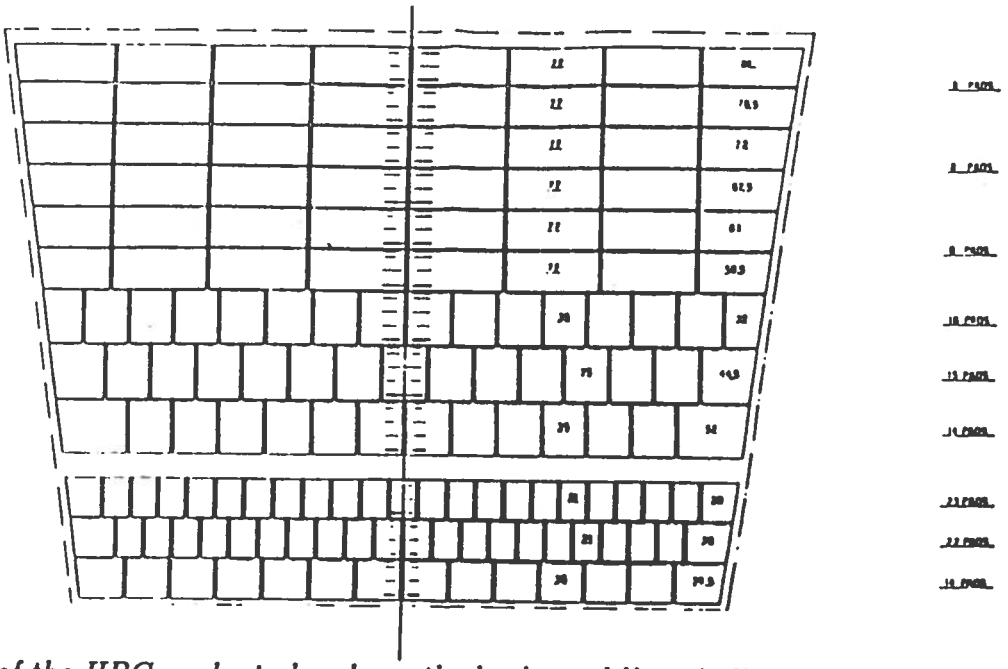

Fig.1 Pad layout of the HPC readout chambers; the horizontal lines indicate the positions of the sense wires.

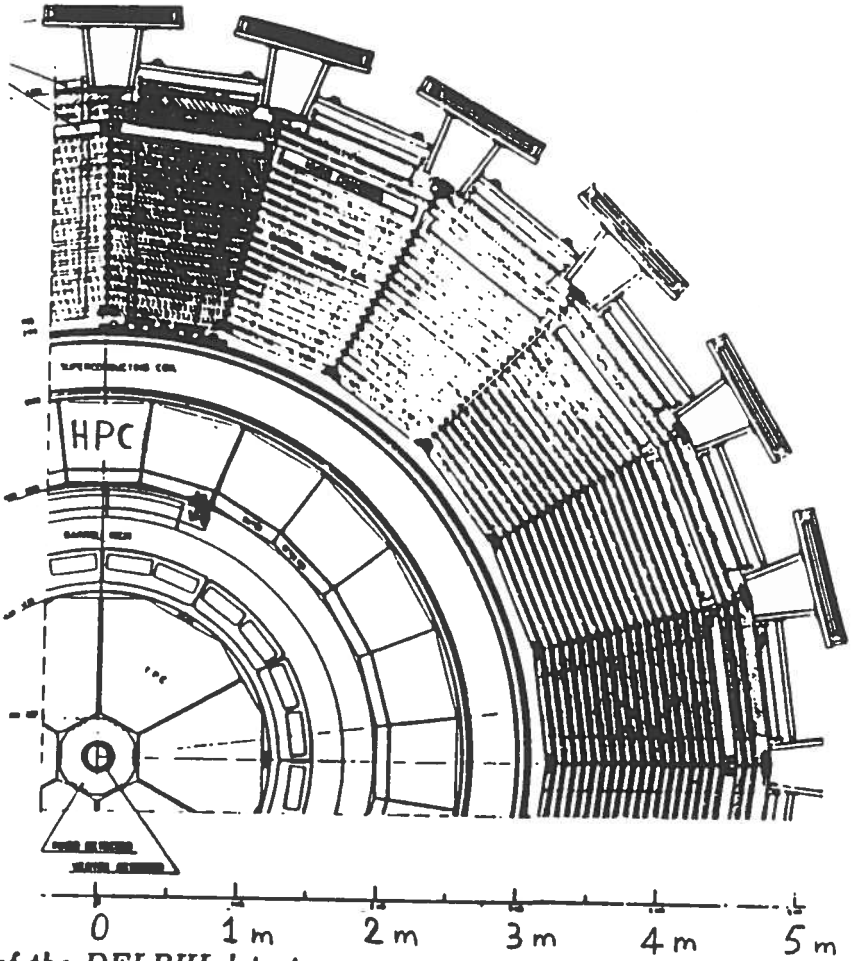

Fig.2 Cross section of the DELPHI detector.

As shown in Fig. 2, the Φ granularity corresponds quite well to the Φ trigger segmentation of the

other detectors in DELPHI with the only remark that, due to the 7.5° rotation of the HPC relative to the Hadron calorimeter (implemented to avoid the alignement of dead space regions), one hadron calorimeter hypertower must match two HPC modules. On the contrary, as shown in Fig. 3 , along Θ the HPC modules do not correspond to the projective segmentation of the Hadron calorimeter.

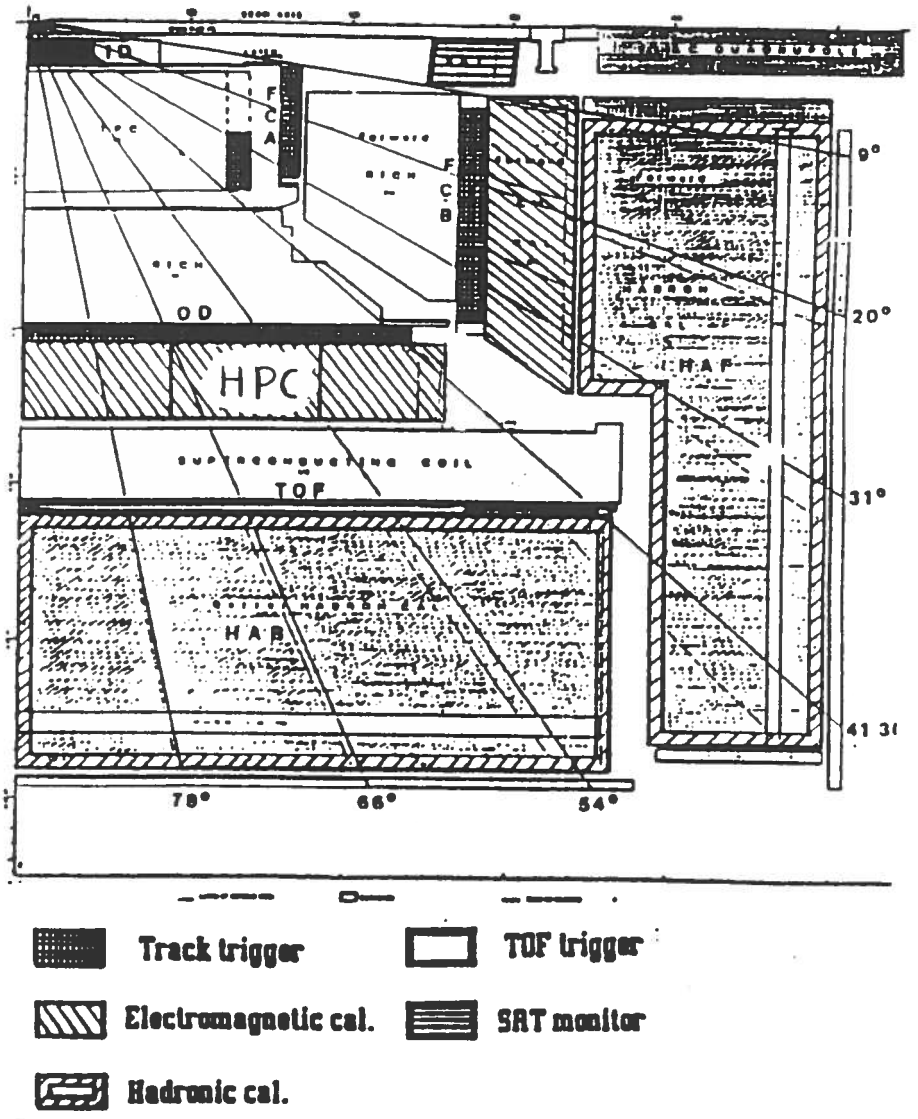

Fig.3 Trigger subdivision along Θ.

To avoid losses in detection efficiency for the showers traversing the non projective boundary between two modules, it was proposed[2] to define projective trigger sectors, matching the hadron calorimeter segmentation, by dividing radially the trigger read-out of the HPC modules in a number of sections and using the drift time information to separate, within each radial section, the various trigger sectors. The principle of this method is schematically shown in Fig. 4. The anode wires or the cathode pads are grouped to form a number of independently read-out radial section. Then, for each section, the energy released in a given trigger sector is proportional to the integral of the current

signals over an appropriatelly defined drift time interval. As shown in Fig. 5, a projective

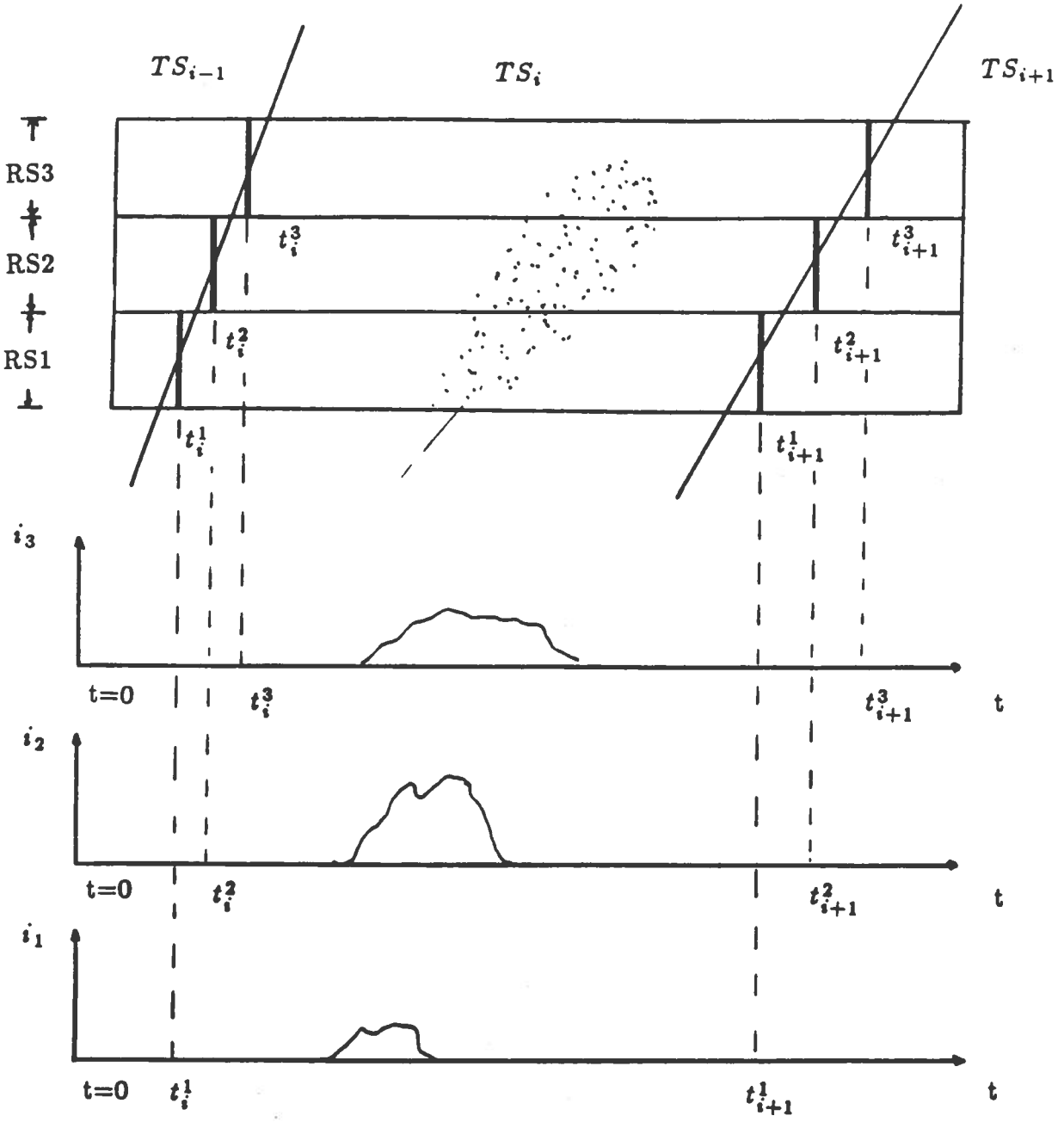

$$E(TS_i) \propto Q(TS_i) = \int_{t_i^1}^{t_{i+1}^1} i_1 dt + \int_{t_i^2}^{t_{i+1}^2} i_2 dt + \int_{t_i^3}^{t_{i+1}^3} i_3 dt$$

Fig.4 Definition of projective trigger sectors for the HPC second level trigger.

segmentation along Θ may than be achieved by adding all the contributions to the various trigger sectors:

$$ETS(1) = TS(1,1,1) + TS(1,2,1) + TS(1,3,1)$$

$$ETS(2) = TS(1,1,2) + TS(1,2,2) + TS(1,3,2) + TS(2,1,2) + TS(2,2,2) + TS(2,3,2)$$

$$ETS(3) = TS(2,1,3) + TS(2,2,3) + TS(2,3,3)$$
$$+ TS(3,2,3) + TS(3,3,3)$$
$$ETS(4) = TS(2,1,4) + TS(3,1,4) + TS(3,2,4)$$
$$+ TS(3,3,4)$$

where $ETS(k)$ is the total energy released in trigger sector k and $TS(i,j,k)$ is the charge collected in the time interval relative to the trigger sector k in radial section j of HPC module i.

A possible method to integrate the charge sampled from a radial section over given drift time intervals is illustrated in Fig. 6 for radial section j of module i which is subdivided in trigger sectors $(k-1)$, k and $(k+1)$.

At the event time the FADC's sampling starts and the digitized value of each sampling is added to the content of a register (set initially to zero) and stored again in the same register. After the last sampling corrisponding to trigger sector $(k-1)$ the output from the adder is stored in a second register and the first one is cleared.

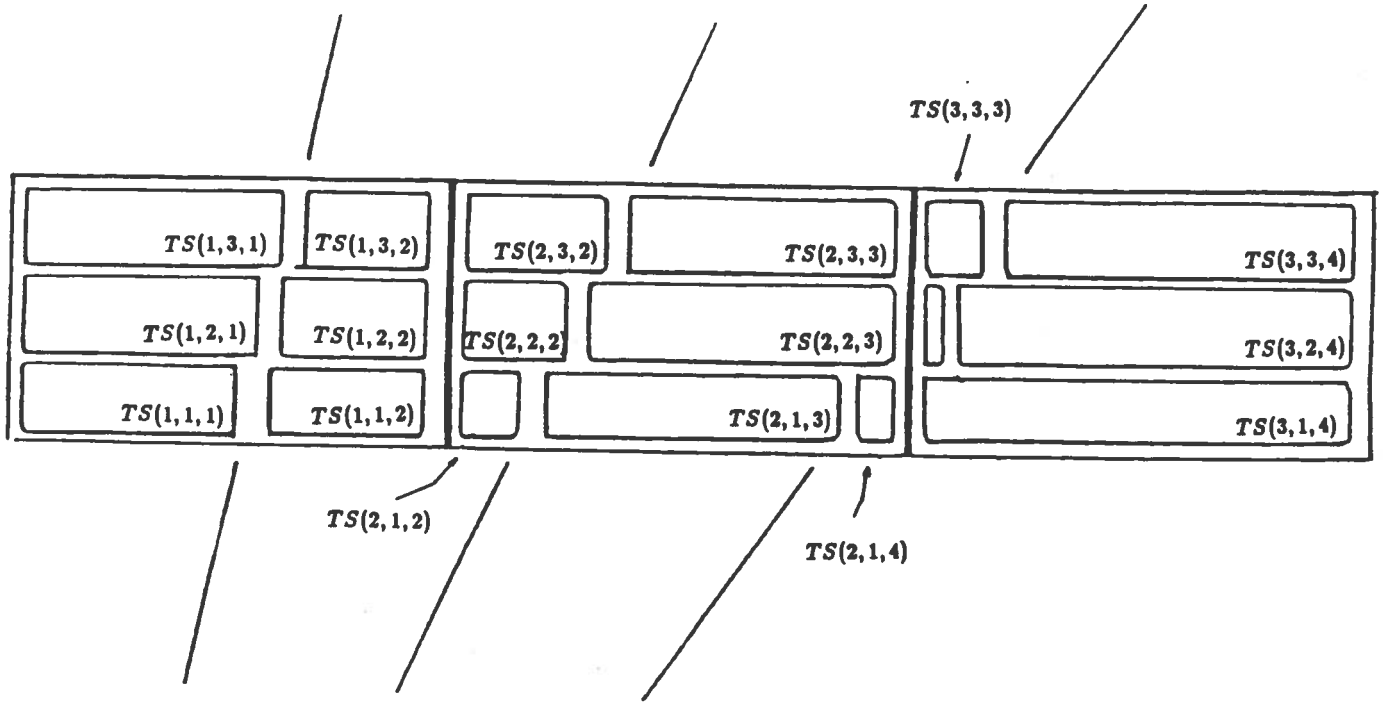

Fig.5 Subdivision of the modules in radial sections for the measurement of the energy released in each trigger sector.

The process continues for trigger sector k and $(k+1)$ until all the drift time elapses; the contents of the registers corresponding to the same trigger sector of the various radial sections may then be added together to define the energy released in a given trigger sector.

The purpose of this paper is first to study the feasibility of such a system by investigating via Monte Carlo simulation how well the HPC trigger sectors, defined as outlined above, approximate the required trigger segmentation as a function of two parameters, which influence the complexity of the system, i.e.:

- the number of radial sections into which a module must be sudvided;

- the sampling frequency.

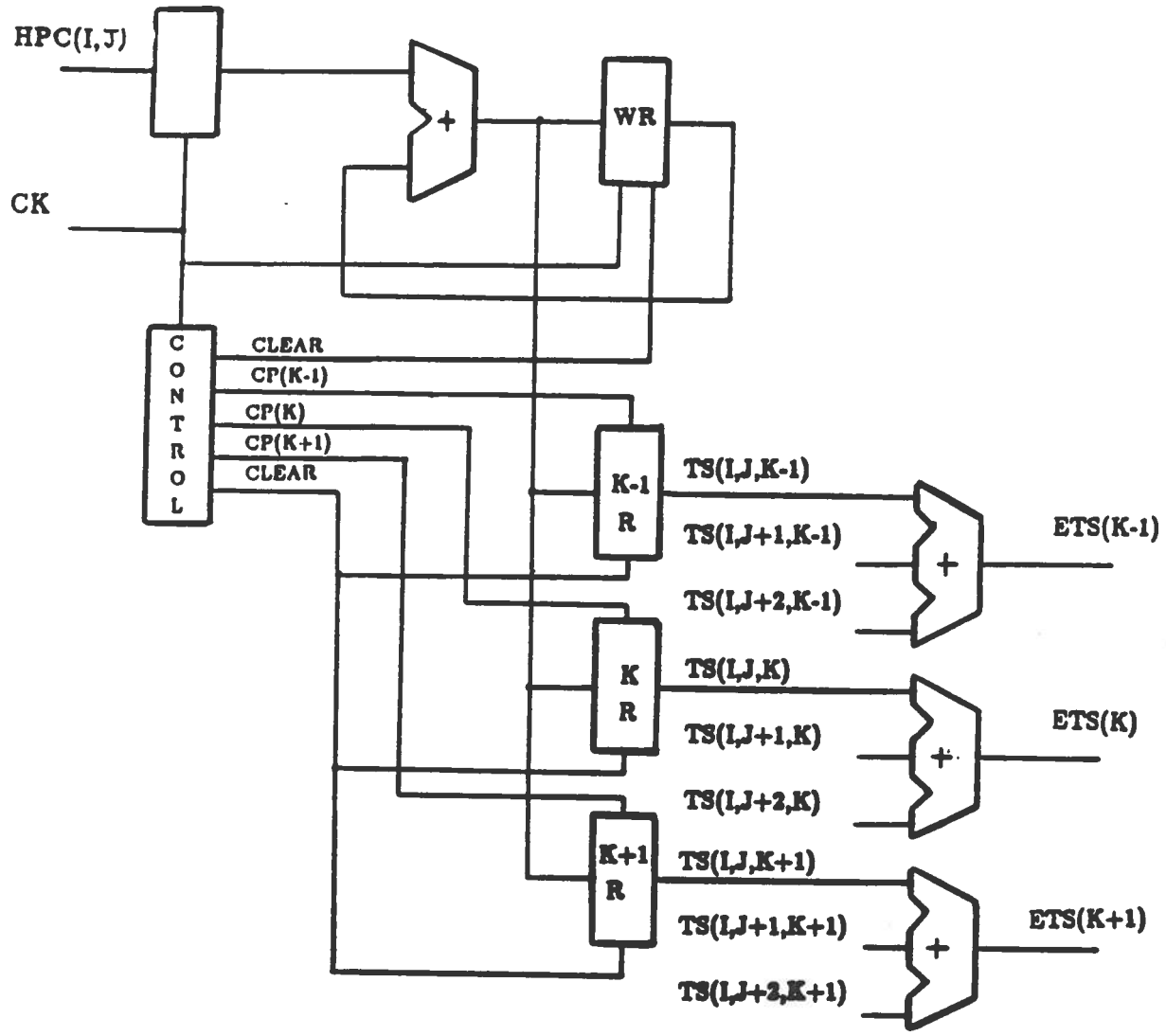

Fig.6 Logical scheme of a circuit to measure the energy released in a trigger sector by summing up the contributions from three radial sections.

In the second place we compare the trigger sector scheme resulting from this study with the originally proposed module granularity in terms of their detection efficiency.

2 - THE MONTE CARLO SIMULATION OF ELECTROMAGNETIC SHOWERS IN THE HPC

The development of electromagnetic showers in the HPC detector has been simulated by using the EGS4 program[3,4,5] with a 1.2 *Tesla* magnetic field and a low energy cut-off of 1.5 MeV for electrons and 0.1 MeV for photons.

The HPC modules[6] were approximated by 39 gas gaps ($80\%Ar, 20\%CH_4$) 0.88 cm thick, separated by 0.27 cm thick homogeneous lead layers. The total drift lenght of a module was 85 cm.

The HPC geometry adopted in the simulation, showing the Θ angles corresponding to the trigger segmentation and the angles delimiting the projection from the intersection point of the boundary between two modules, is presented in Fig. 7.

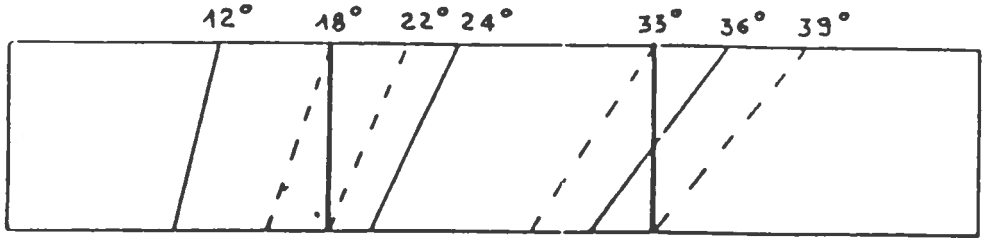

Fig.7 The HPC geometry adopted in the simulation: the continuos lines correspond to the trigger segmentation and the dashed ones define the projection from the intersection point of the boundary between two modules.

The simulated showers were originated by electrons of various energies entering perpendicularly the middle of the coffin in the (r, Φ) plane and with various angles of incidence in the (r, Θ) plane.

The charge distribution along z was binned in 136 cells 0.625 *cm* long corresponding, for a drift velocity of 5 $cm/\mu sec$, to time intervals of 125 *nsec*.

In this way the information on the energy deposition in a module was collected in 5304 (r, z) cells arranged as a bidimensional array of 39 rows and 136 columns,where the rows represent the gas gap and the columns the z-coordinate.

The following data were recorded for each event:

- The energy and the incidence angle of the original particle;
- the modules and trigger sectors which were hit.
- the total energy deposited in each trigger sector and module;
- the number of cells with an energy content different from zero.

Then, for each hit cell, the cell module number, the cell position along r and z and its energy content were recorded.

3 - DEFINITION OF THE TRIGGER SECTORS

Using the data from the Monte Carlo simulation, we have studied how well the projective segmentation in Θ may be approximated with the method outlined in Section 1 as a function of the number of radial sections and of the sampling frequency.

In particular we have considered the case of 2, 3 and 8 radial sections, as shown in Fig. 8, and two values, 125 *nsec* and 500 *nsec*, for the sampling period.

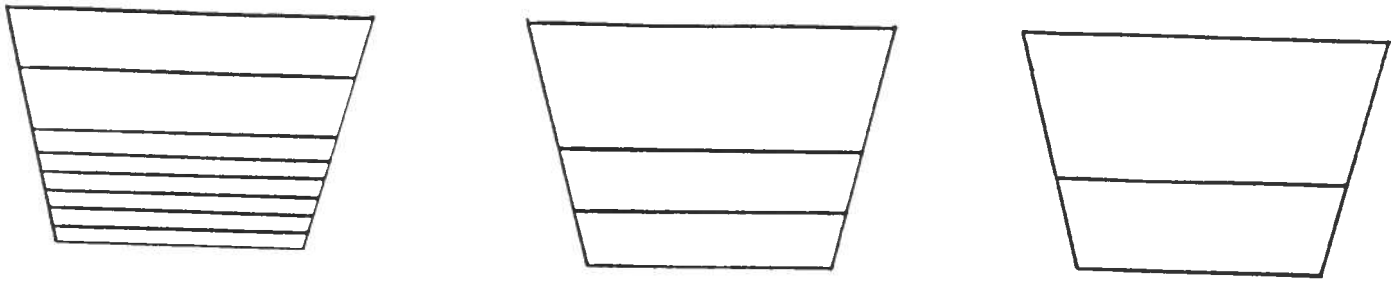

Fig.8 The three radial segmentations studied in this report.

To evaluate the goodness of the approximation we have considered showers originated by electrons of 2, 5 and 10 GeV hitting the detector at angles corresponding to the boundary between the trigger sectors ($\Theta = 12^o, 24^o, 36^o$) and we have calculated the quantity

$$\frac{(E_1 - E_2)}{E}$$

where E is the total energy of the shower and E_1, E_2 are the energies released on the two sides of the approximated border between the two neighbouring sectors interested by the development of the shower: the smaller this quantity, the better the approximation.

The results shown in Fig. 9 suggest that, independently of the number of radial sections, 500 *nsec* sampling is too coarse, especially at small (12^o and 24^o) angles. Grouping the wires or the cathode pads to form two radial sections only with 125 *nsec* sampling is also too coarse at large (36^o) angles of incidence.

The combination of 3 radial sections and of a 125 *nsec* sampling period gives a satisfactory projective trigger topology for all values of Θ. One may notice that using 8 radial sections and 125 *nsec* sampling does not show any improvement with respect to the case of 3 radial sections due to the fact that a sampling period shorter than 125 *nsec* would perhaps be required to take advantage of such a large number of radial sections.

The conclusion of this study is, therefore, that in the energy region of interest for the HPC second level trigger an acceptable approximation of the trigger segmentation in Θ may be achieved by dividing the HPC module trigger read-out into 3 radial sections and sampling the signals from each section at 8 MHz.

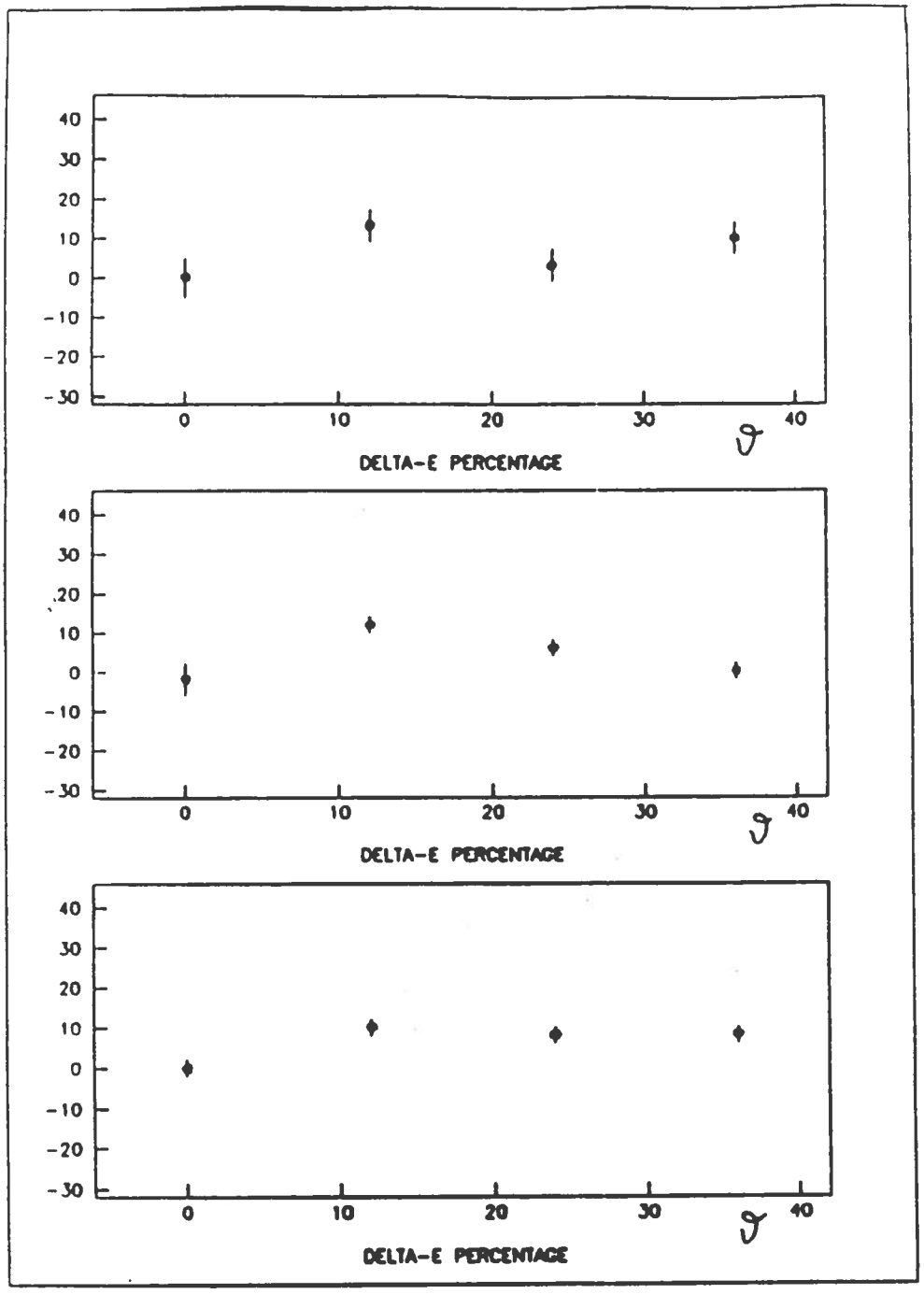

$E_{inc} = 2\ GeV$

$E_{inc} = 5\ GeV$

$E_{inc} = 10\ GeV$

Fig.9a Difference (in percentage) between the energies released in two contiguous trigger sectors by electrons having the sector boundary as incidence direction: 8 radial sections, 125 nsec sampling period.

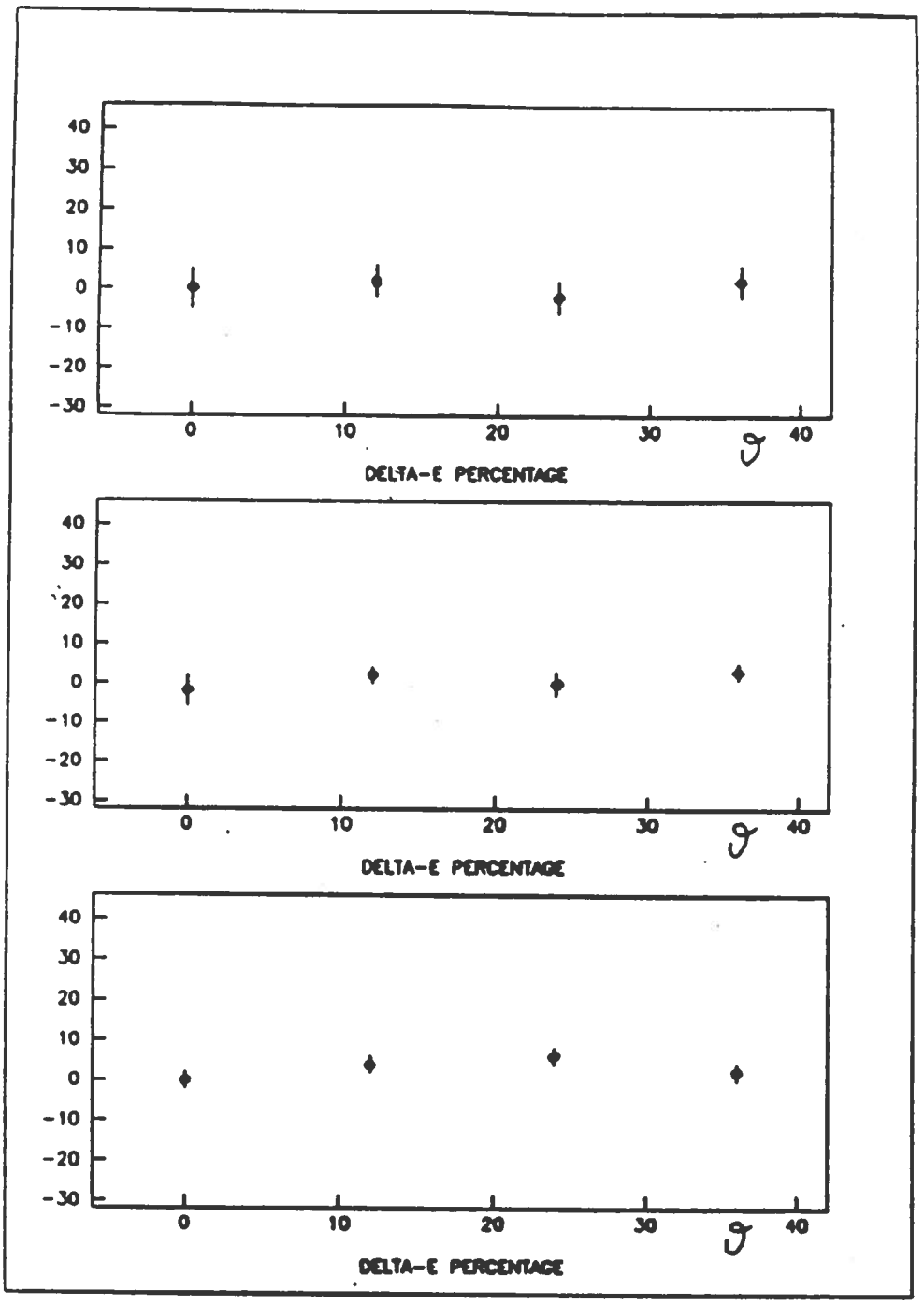

$E_{inc} = 2\ GeV$

$E_{inc} = 5\ GeV$

$E_{inc} = 10\ GeV$

Fig.9b Difference (in percentage) between the energies released in two contiguous trigger sectors by electrons having the sector boundary as incidence direction: 3 radial sections, 125 nsec sampling period.

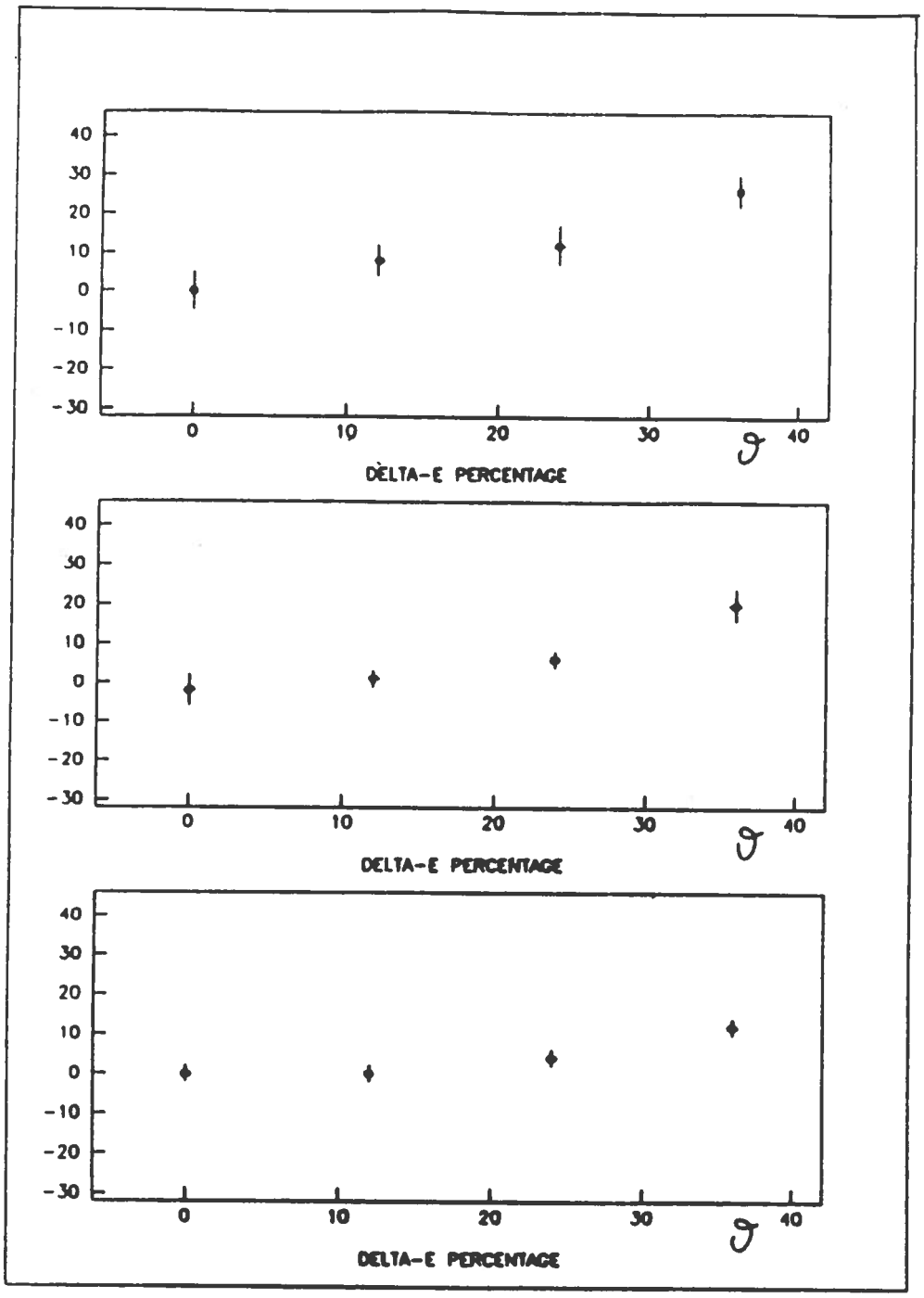

$E_{inc} = 2\ GeV$

$E_{inc} = 5\ GeV$

$E_{inc} = 10\ GeV$

Fig.9c Difference (in percentage) between the energies released in two contiguous trigger sectors by electrons having the sector boundary as incidence direction: 2 radial sections, 125 nsec sampling period.

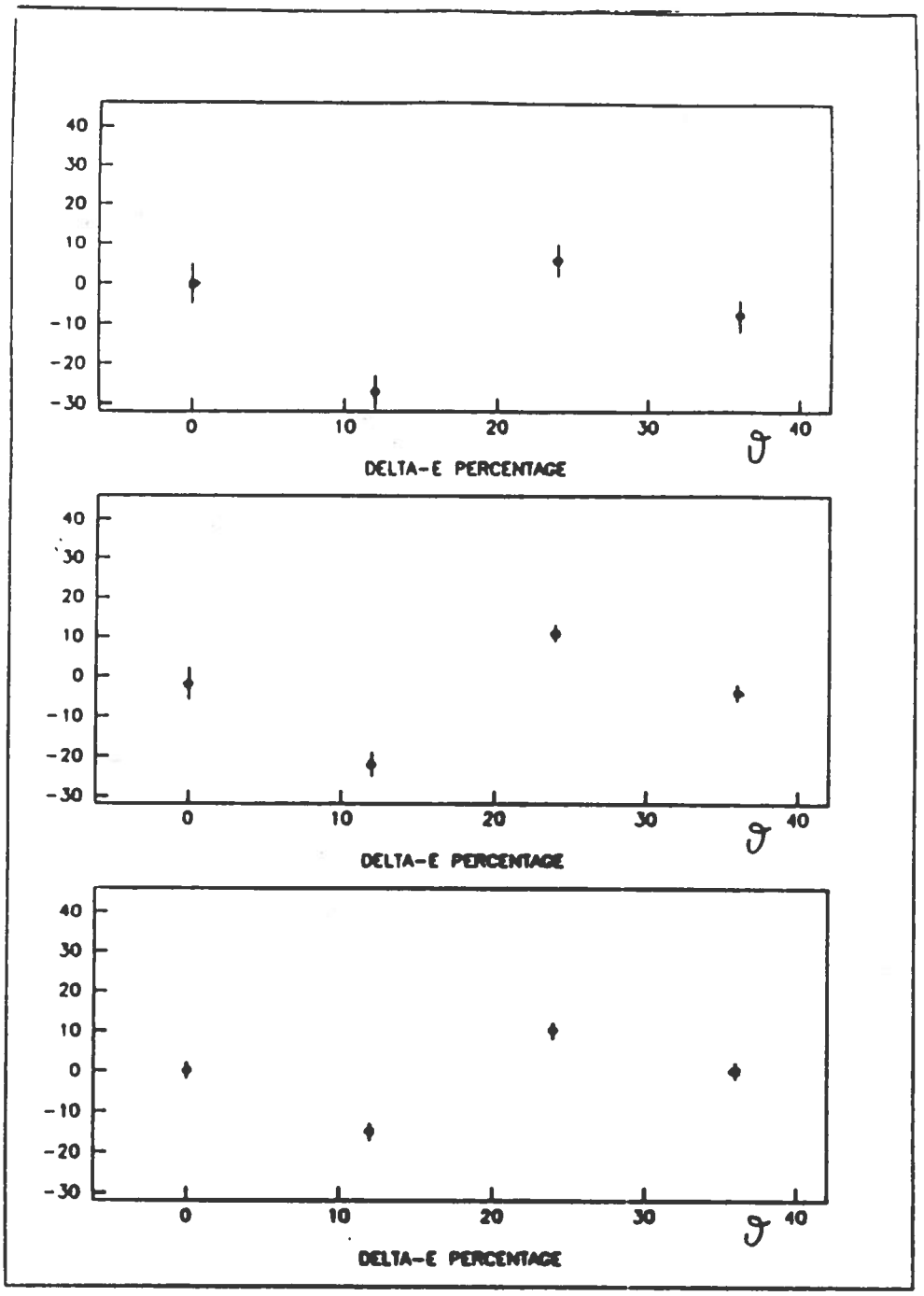

$E_{inc} = 2\ GeV$

$E_{inc} = 5\ GeV$

$E_{inc} = 10\ GeV$

Fig.9d Difference (in percentage) between the energies released in two contiguous trigger sectors by electrons having the sector boundary as incidence direction: 8 radial sections, 500 nsec sampling period.

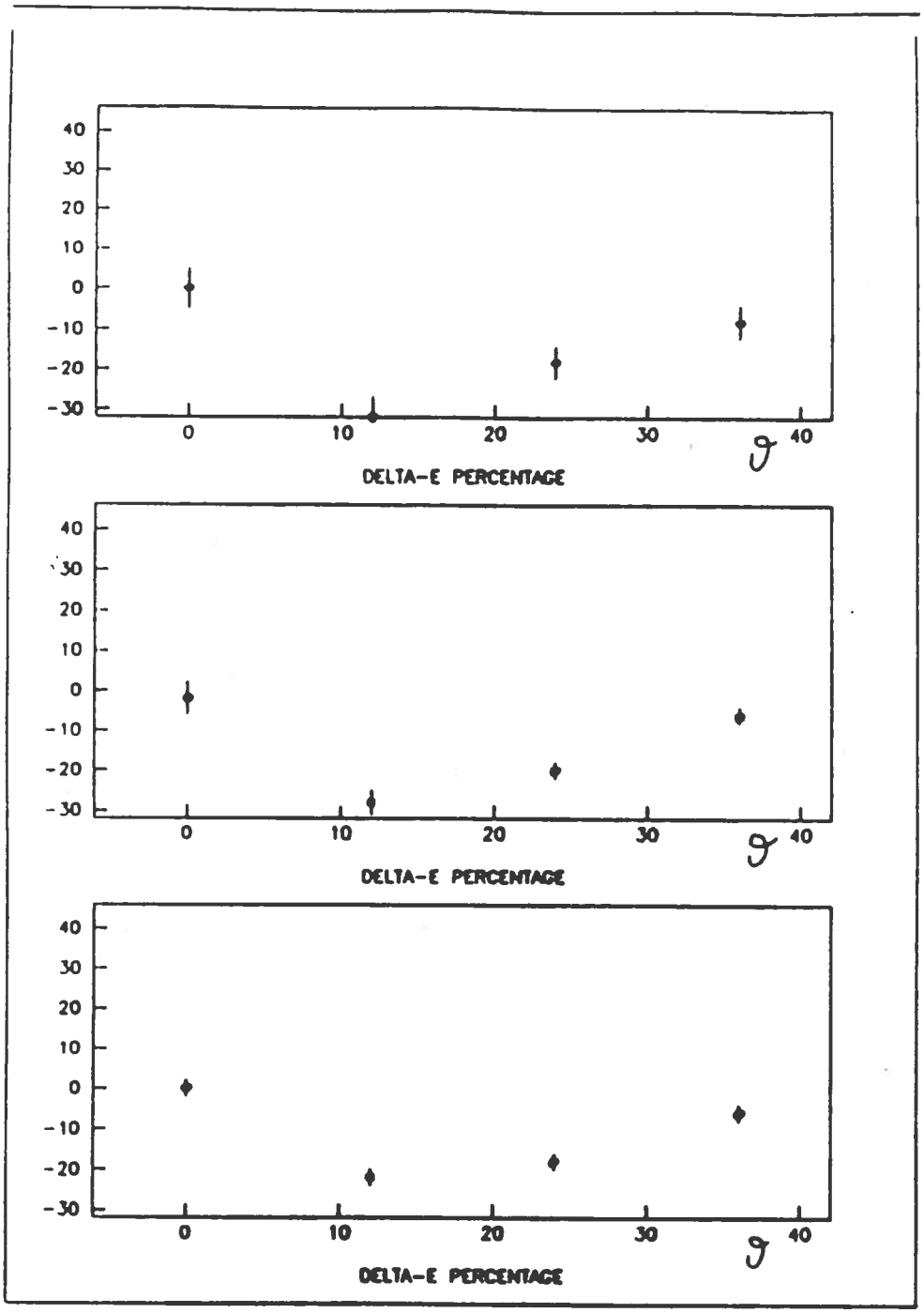

$E_{inc} = 2\ GeV$

$E_{inc} = 5\ GeV$

$E_{inc} = 10\ GeV$

Fig.9e Difference (in percentage) between the energies released in two contiguous trigger sectors by electrons having the sector boundary as incidence direction: 9 radial sections, 500 nsec sampling period.

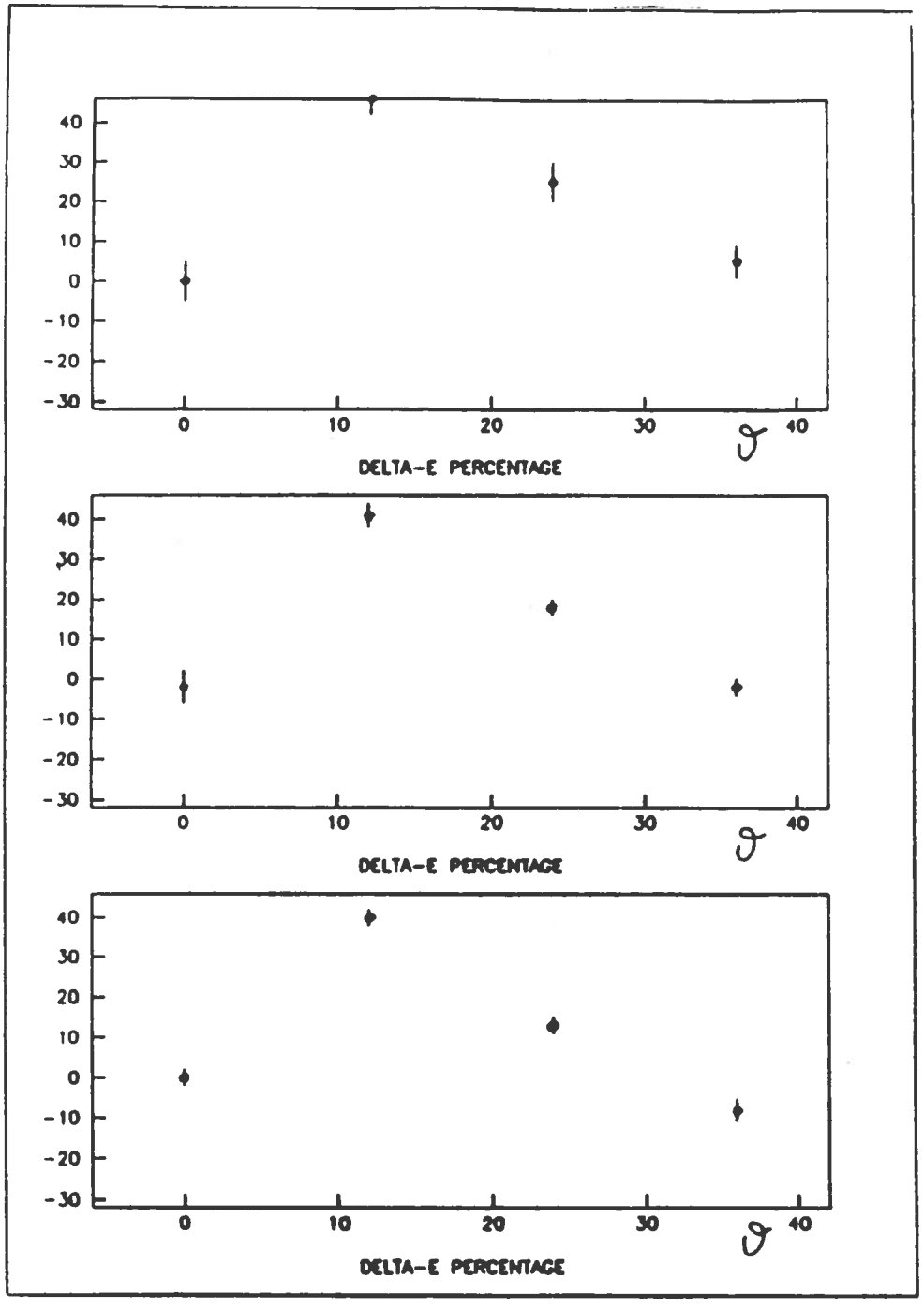

$E_{inc} = 2\ GeV$

$E_{inc} = 5\ GeV$

$E_{inc} = 10\ GeV$

Fig.9f Difference (in percentage) between the energies released in two contiguous trigger sectors by electrons having the sector boundary as incidence direction: 2 radial sections, 500 nsec sampling period.

4 - TRIGGER SECTORS VERSUS MODULES: A COMPARISON IN TERMS OF EFFICIENCY

Some fraction of the energy released by showers originated by particles hitting the detector near the boundary of a trigger sector spills over to the neighbouring trigger sector, causing a reduction of the trigger efficiency when a fixed energy threshold is used. On the other hand, obviously, when a fixed energy threshold is applied to the energy measured in a whole HPC module there will also be a trigger inefficiency when the shower developes across two modules.

We have quantitatively studied this effect both for the trigger sector and for the module segmentation by simulating showers originated by electrons impinging on the detector with various Θ angles corresponding to the border zones and energy of 2 and 5 *GeV* corresponding to the expected values for the low and high energy thresholds.

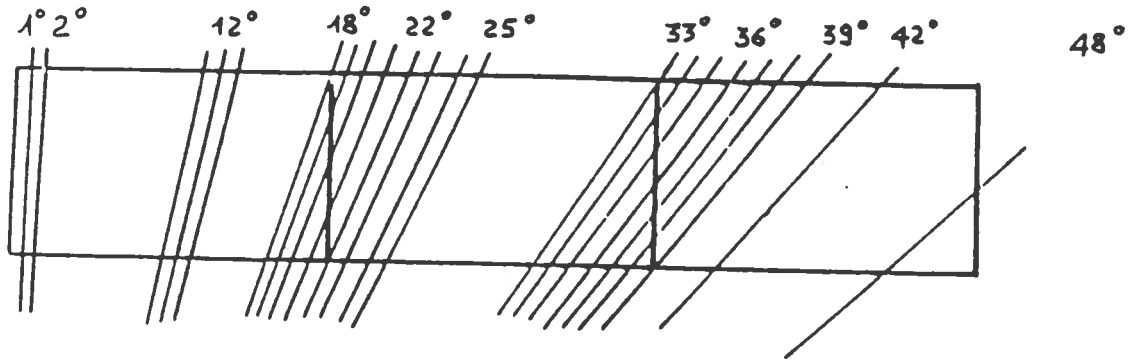

Fig.10 Electron incidence angles used in the simulation: they cover the regions around the sector boundaries and around the module boundaries.

Fig. 10 shows schematically the geometry adopted in the Monte Carlo and the angles of incidence of the electrons. The trigger sectors have been defined, as suggested by the results discussed in section 3, by adopting 3 radial subdivisions and a 125 *nsec* sampling period.

Fig. 11 shows the ratio between the energy observed in a trigger sector and the incoming energy, E^{TS}_{obs}/E_{inc}, as a function of the angle of incidence, Θ. The inefficiency at the trigger sectors boundary ($\Theta = 0^o, 12^o, 24^o, 36^o$) is very clear, but the angular region where the E^{TS}_{obs}/E_{inc} ratio drops below the plateau level is quite narrow: $\pm 1^o$ around the boundary angle.

The resulting trigger efficiency defined as the ratio between the number of simulated events in which at least one of the trigger sectors measures an energy greater than the trigger energy threshold and the total number of events, is shown in Fig. 12 as a function of energy threshold for the case of 5 *GeV* electrons and the worst incidence angles, i.e. those angles at which the incident energy is shared equally between the two trigger sectors.

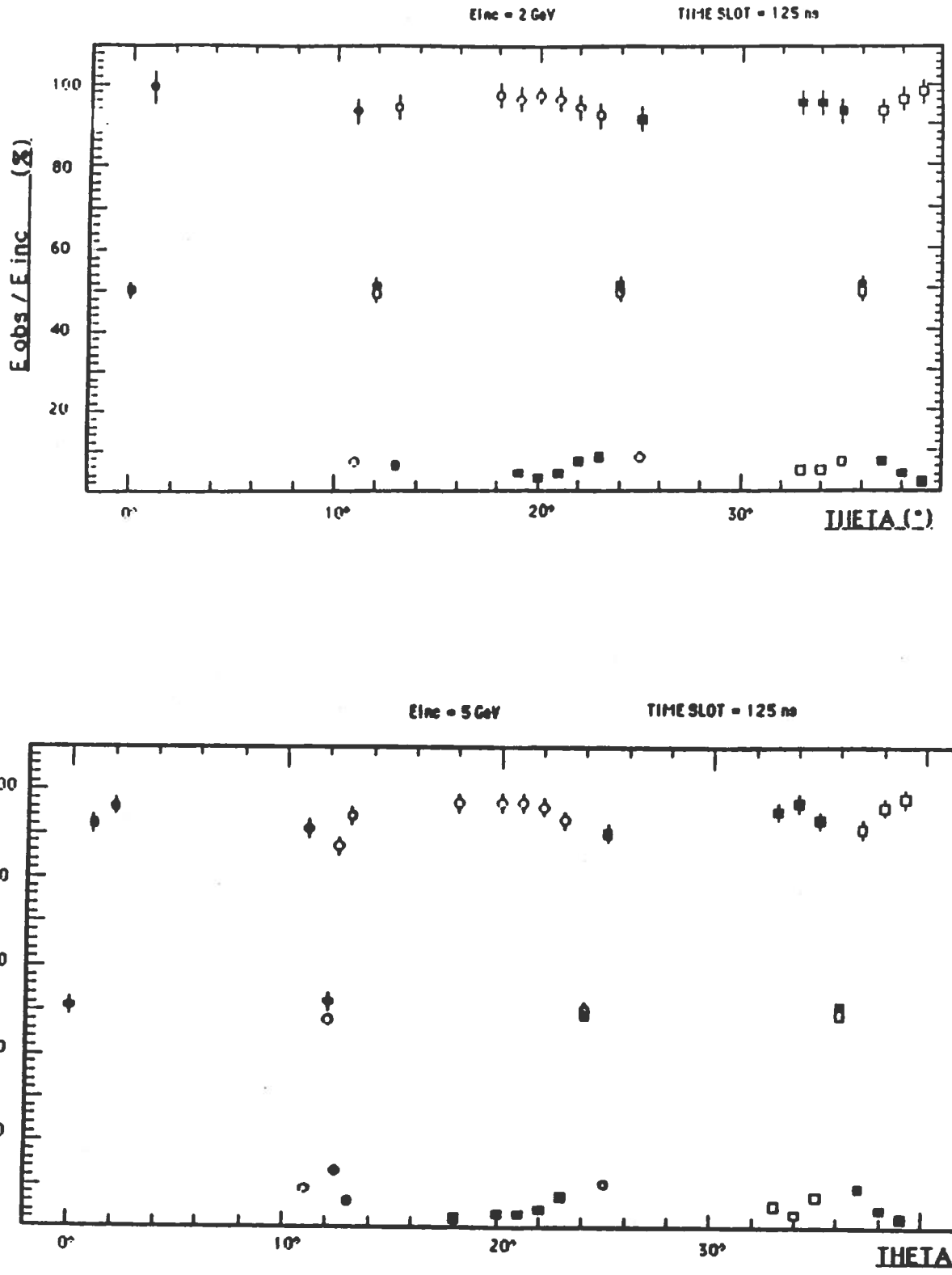

Fig.11 Incident energy fraction observed in each trigger sector, as a function of the incidence angle (• ≡ 1st sector; ○ ≡ 2nd sector; ■ ≡ 3rd sector; □ ≡ 4th sector). The sectors are defined by means of three radial sections.

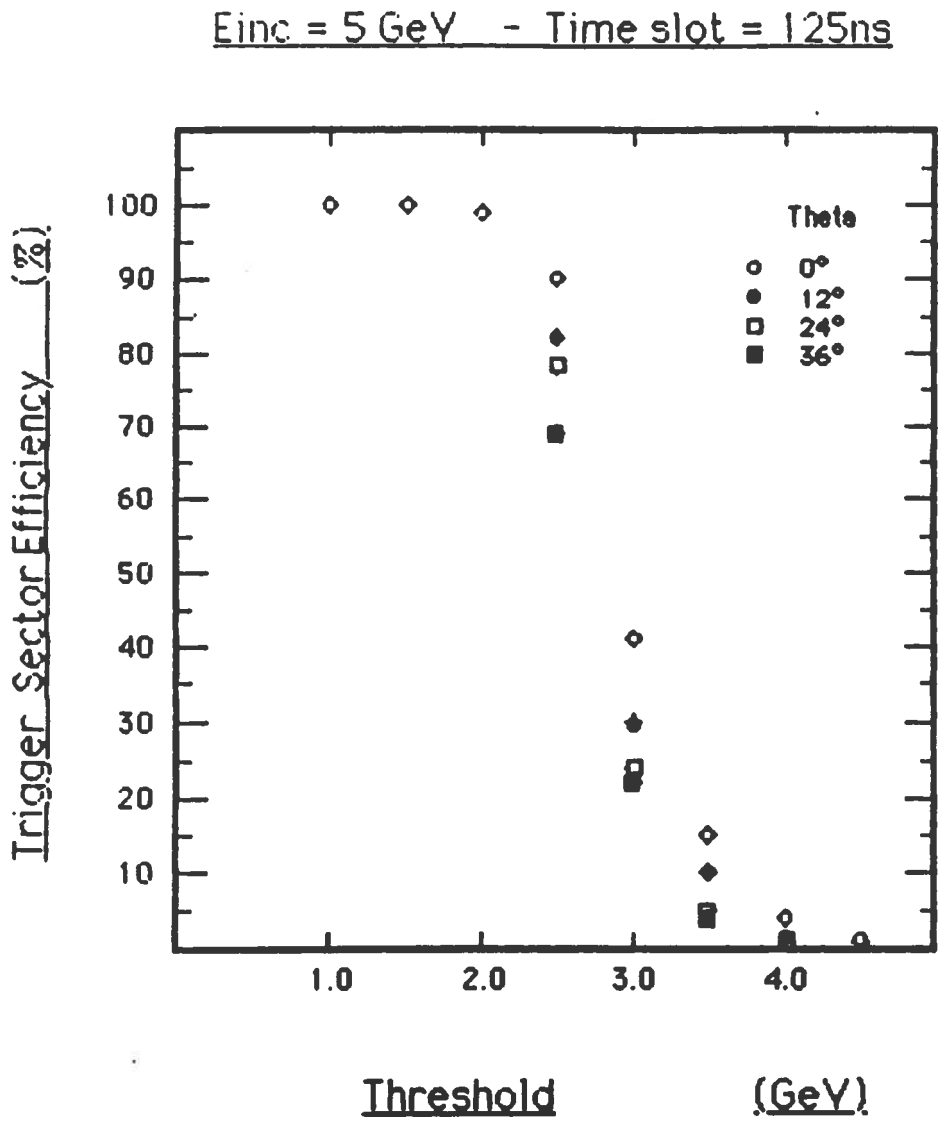

Fig.12 Trigger efficiency as a function of the applied energy threshold for all the angles corresponding to the sector boundaries (sector scheme).

Fig. 13 shows the ratio between the energy observed in a module and the incoming energy, E_{obs}^{mod}/E_{inc}, as a function of the incidence angle. Also in the case of the 3 separate module segmentation an inefficiency region is clearly observable and is somewhat wider in Θ than for the trigger sector scheme. In fact the region where the ratio E_{obs}^{mod}/E_{inc} starts to decrease with respect to the plateau level extends over $\pm 2^{\circ}$ around the angle at which the two modules share equally the incident energy.

The resulting trigger efficiency, defined as the ratio between the number of events in which at least one of the modules measures an energy greater than the trigger threshold and the total number

is shown in Fig. 14 as a function of the energy threshold for 5 *GeV* electrons and the worst incidence angles.

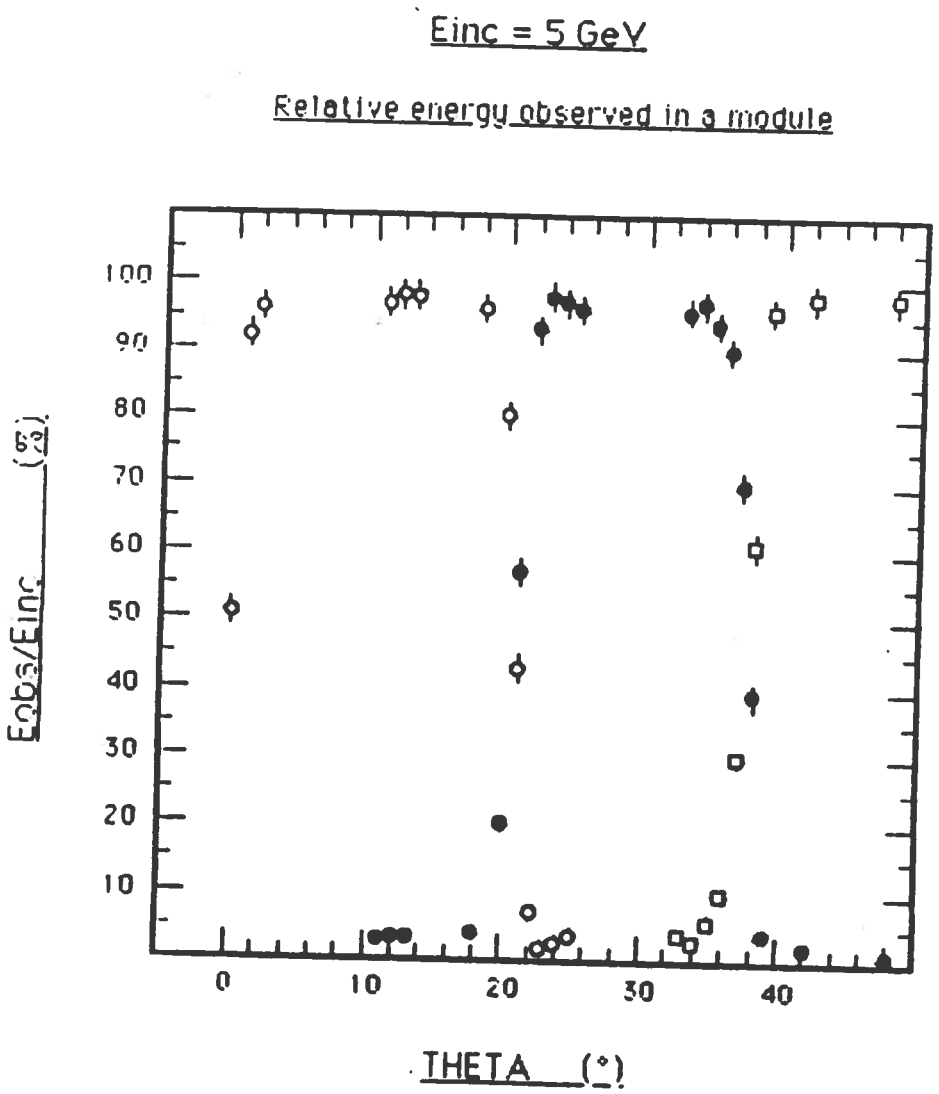

Fig.13 Incident energy fraction observed in each module, as a function of the incidence angle (o ≡ 1st module; • ≡ 2nd module; □ ≡ 3rd module).

5 - CONCLUSIONS

The results discussed in Section 3 show that a trigger segmentation in Θ finer than the HPC modularity and matching the segmentation dictated by the hadron calorimeter hypertowers and by the other detectors may be achieved by grouping the wires or the pads of the modules into at least three radial sections and sampling the drifted charge every 125 *nsec* or less.

The results presented in Section 4 show however that there is marginal improvement in the overall efficiency for the projective trigger sector solution compared to the module scheme.

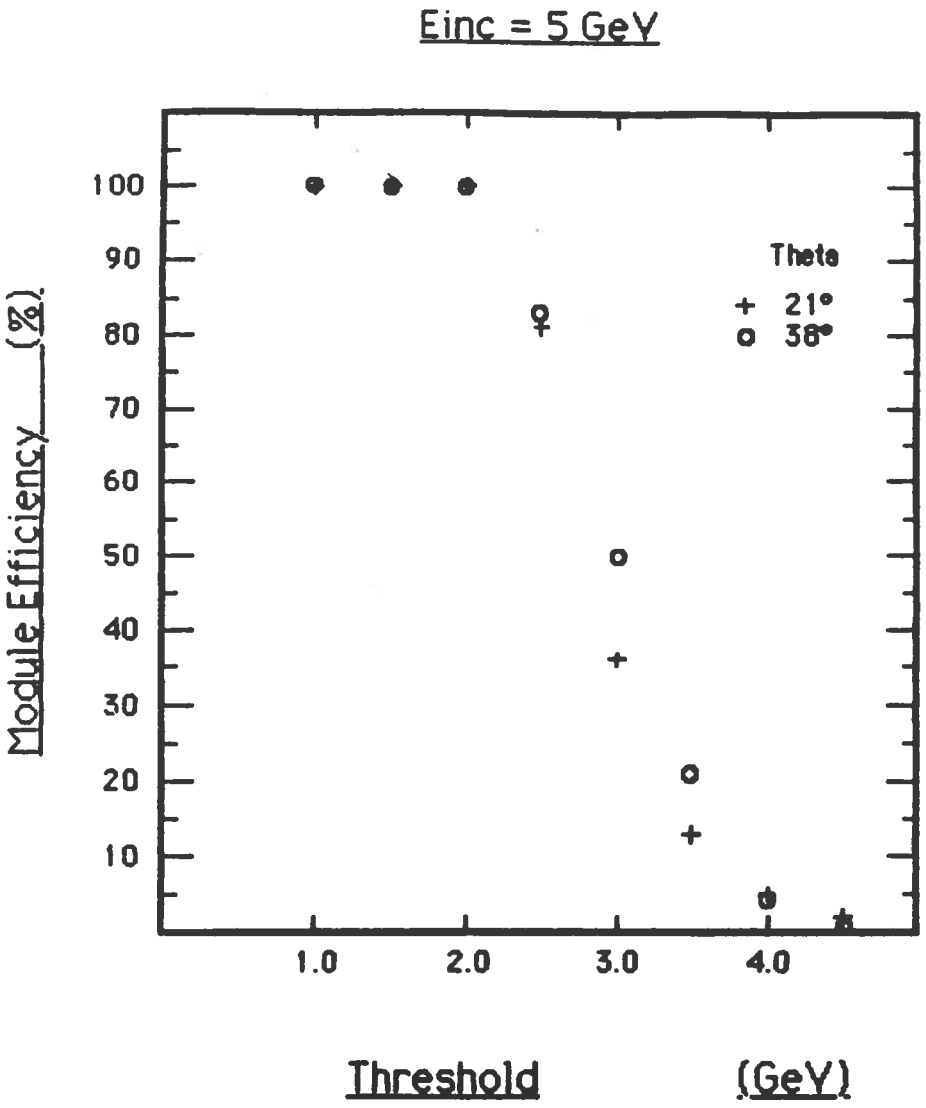

Fig.14 Trigger efficiency as a function of the applied energy threshold: the 21° direction crosses the boundary between the 1st and the 2nd module, the 38° direction crosses the boundary between the 2nd and the 3rd module (module scheme).

In fact, as shown in Fig. 15, the geometrical solid angle $\Delta\omega/\omega$ over which the detection efficiency is greater than a given limit does not differ dramatically for the two cases. In view of the above discussion, adoption of the sector scheme would be more for the sake of conformity rather than to improve efficiency. On the other hand, the module scheme lends itself to a much simpler implementation than the trigger sector scheme. In fact, it does not require, in principle, the partitioning of the trigger module read-out into thee radial sections and collection of the charge over several separate drift time intervals.

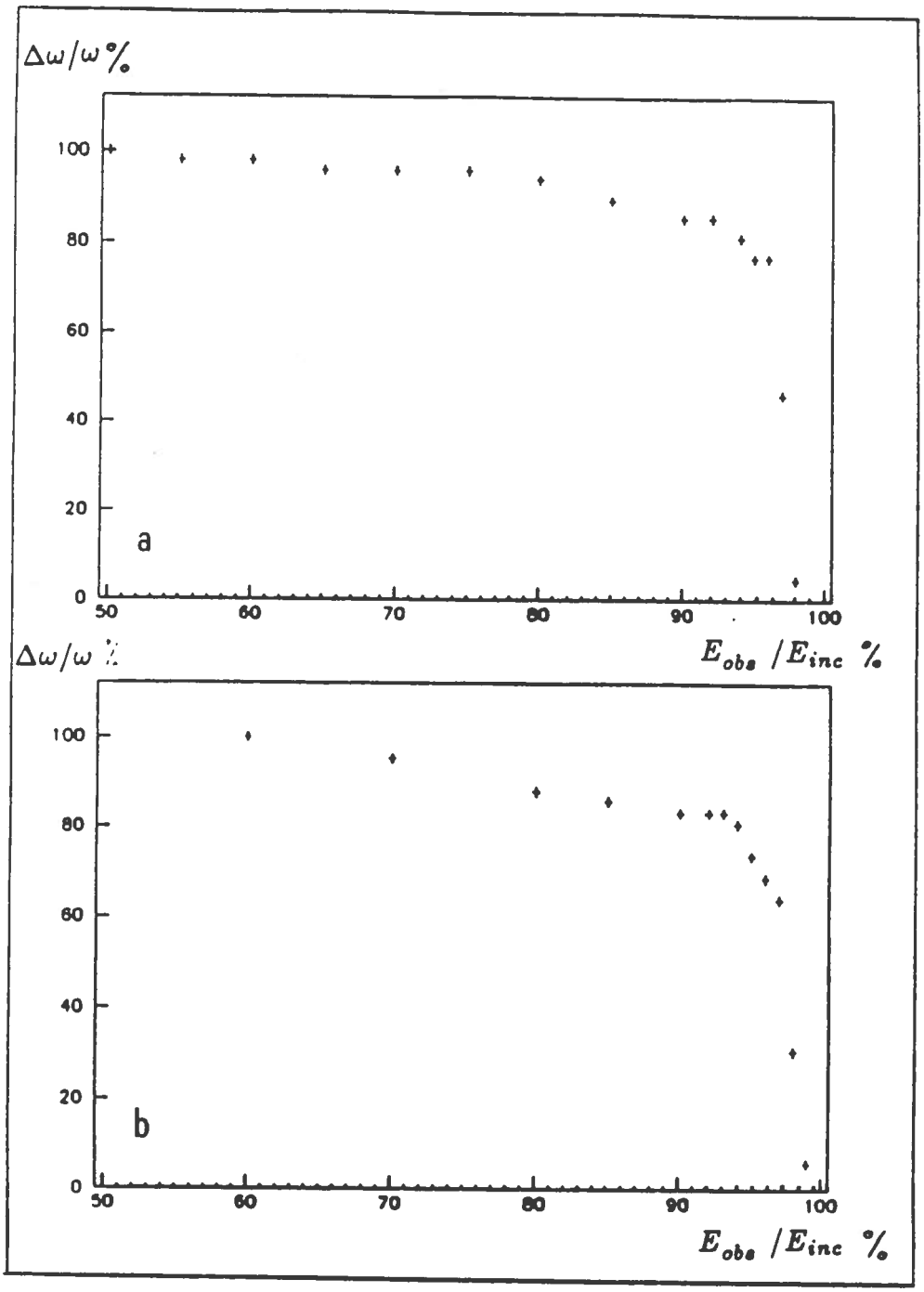

Fig.15 Solid angle fraction over which an electron can hit the HPC, so that a given fraction of its energy is measured by the module trigger system (a) and by the sector trigger system (b)

6 - REFERENCES

(1) a) T.W. Meyer. HPC Trigger Group, May 10, 1984, b) F. Udo DELPHI 84-35 DAS-3, June 8, 1984.
(2) A. Cattai, P. Montanari, P. Giusti, N.Yamdagni. Contributions to the HPC meetings, January - April, 1985.
(3) R.L. Ford, W.R. Nelson, The EGS Code System, SLAC Report No. 210 (1978).
(4) For the simulation of electromagnetic showers we used the version of the EGS4 program adapted to the HPC and written in Fortran 77 by H. Burmeister.
(5) D. Bollini, C. Chiccoli, P.Pasini, DELPHI 85-52 PROG-28, 19th June, 1985.
(6) a)F.L. Navarria. Nucl. Instr. Meth. **A257**, 499 (1987), b) A. Cattai et al., Nucl. Instr. Meth. **A235**, 310 (1985).